Proceedings of the ASME 2016 International Mechanical Engineering Congress and Exposition
IMECE2016
November 11-17, 2016, Phoenix, Arizona, USA

IMECE2016-65221

Calibration of a Design Tool for Dynamic Characteristics of Gas Labyrinth Seals

R. Gordon Kirk
Virginia Tech
Blacksburg, Virginia, USA

Wen Jeng Chen
Eigen Technologies, Inc.
Davidson, NC, USA

ABSTRACT

The analysis of all critical path high pressure machinery must include the account of the influence of the gas labyrinth seals. This paper reviews the prior work on labyrinth seal analysis starting in the 1980's. The discussion gives a summary of the calibration of the bulk flow analysis to CFD results for a number of conditions. The calibration process was conducted over the last decade and the current paper presents the key results needed to justify the use of this bulk flow analysis for design of machinery with bladed labyrinth seals. A new design tool is discussed with illustrations of the type of seals that can be studied. The dynamic characteristics calculated using the labyrinth seal program can be used in rotordynamic analysis programs to predict the change in system stability produced by the gas labyrinth seals.

INTRODUCTION

The analysis of all critical path high pressure machinery must include the influence of the gas labyrinth seals. The bulk flow analysis of labyrinth seals including dynamic stiffness and damping characteristics was first published in the 1980 conference paper by Iwatsubo [1]. The work by Childs and Scharrer in the mid 1980's [2-5] extended and clarified the Iwatsubo analysis. The journal paper [2] was presented in May of 1984 at a NASA workshop held at Texas A&M. That conference paper had the outline of the bulk flow process but the leakage calculation was not provided. The first author was working for a compressor company and the need for analysis of labyrinth seal influence on compressor stability was highly desired. A complete derivation of the required equations was made and programmed. The first order leakage flow routine was developed and the analysis was compared to existing leakage data available at that time. The analysis was applied to a full load compressor test that gave confidence that the calculations were acceptable for prediction of instability in centrifugal compressors [6, 7]. From the beginning, the labyrinth seal analysis program was developed for design studies. Every chamber of the seal has the friction factors and geometry specified and the leakage routine could be corrected to test data by using the flow correction parameter (FC). A unique feature was the ability to model the leak path from the tip of the impeller down the back or front of the disk and through the labyrinth seal [8]. Both step down and step up seals with teeth on rotor or on stator or interlocking, was provided. The initial computer program was written in Fortran and a formatted card image input of data was the best option at that time.

The first PC-based rotor analysis programs [9] could calculate both forced response and stability, and included fluid-film bearings, oil seals, turbulent seals for pumps, and gas labyrinth seals for compressors and turbines. These programs were all Fortran based with preprocessors written in PASCAL. In the late 1980's, PASCAL was the program of choice for preprocessors. Unfortunately, that was a very bad idea since the preprocessors will not support Windows 7 or higher. The good news is that the labyrinth seal analysis can be called from a modern pre-processor without the need to re-write the analysis code.

Most attempts to produce a better bulk flow analysis by considering multiple volumes in the chambers were not acceptable for design work, to the authors' knowledge. The best solutions are those from CFD analysis, but this comes with a huge difference in the solution time and level of difficulty to model the seal systems [10-16]. The better solution would be a simple bulk flow analysis calibrated to specific machinery conditions or an analysis that is very likely to provide a worst case result for predicting stability. The results of a series of research projects [16-20] using the best available CFD calculation procedures included comparisons to the leakage and force levels predicted by the bulk-flow program [7, 8]. The following discussion gives a brief summary of the pertinent results that were found in those CFD studies. These results can be used to better understand the strengths and weakness of applying bulk-flow analysis for labyrinth seals.

 Copyright © 2016 by ASME

SUMMARY OF CFD STUDIES

The paper by Hirano et al [16] discussed one of the first labyrinth seal solutions from the commercial CFD program TASCflow, and the results were compared to the bulk-flow program, referred to as DYNLAB [7]. Hirano did a complete grid study prior to generating the comparison study results. In general the conclusion was that DYNLAB results were pessimistic for all the conditions studied for a 5 tooth compressor eye seal and a 20 tooth turbine seal. The pressure drop for the compressor eye seal using the CFD program TASCFlow, is compared to the DYNLAB bulk-flow results in Fig 1. The parameters for this seal are provided in Appendix Table A-1.

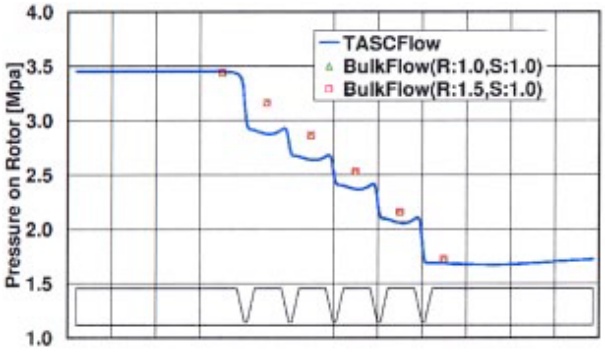

Fig 1 Pressure distribution for 5 tooth compressor eye seal [16]

The calculation of the force levels was made using a rotating reference frame to allow a steady state solution of the rotor whirling about the center position. After solutions with various whirl speeds (Ω) are obtained, the seal force of each case is calculated by integrating the pressure on the rotor. Assuming the effect of inertia is negligible, the dynamic coefficients are derived from the following equations.

$$\left.\begin{aligned} F_r/\delta &= -K - \Omega c \\ F_t/\delta &= k - \Omega C \end{aligned}\right\} \quad (1)$$

where

K : direct stiffness
k : cross-coupled stiffness
C : direct damping coefficient
c : cross-coupled damping coefficient
F_r : seal force in radial direction
F_t : seal force in tangential direction
δ : eccentricity

and

Q eff = k–(whirl frequency) x C (2)

Figure 2 (a) and (b) show the relation between the seal force and whirl speed. The seal force in the tangential direction by TASCflow is close to those by the bulk flow program (DYNLAB), though there is some difference for the results in the radial direction. The predicted seal forces by TASCflow are smaller than those by DYNLAB. The inertia coefficients in both directions are negligible since each curve is almost a straight line.

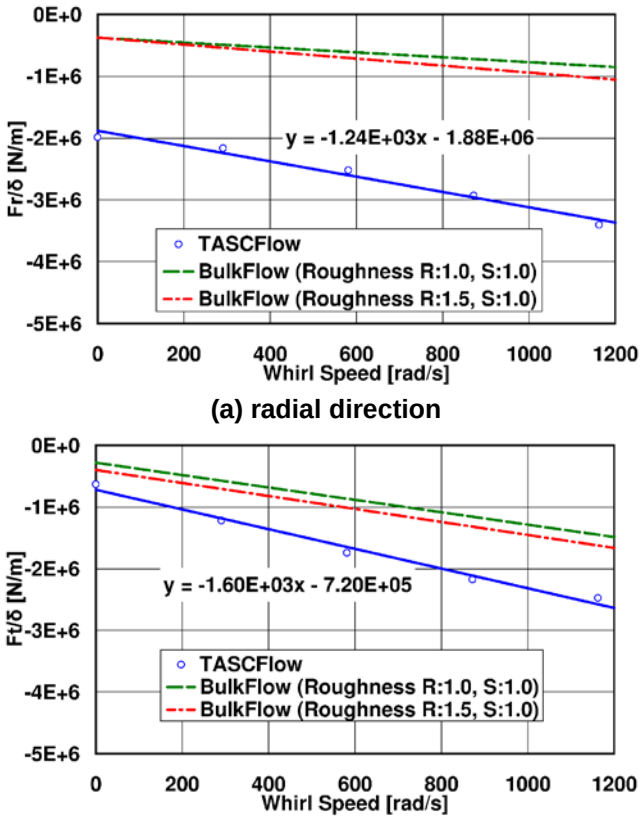

Fig 2 Force levels for the 5 tooth compressor eye seal [16]

Figure 3 shows the average swirl in each chamber of a 20 tooth turbine seal. This graph includes a result by TASCflow and 4 results by the bulk flow program [7] with various global surface roughness parameter multipliers. In the graph R means the relative roughness of the rotor surface and S means the relative roughness of the stator surface.

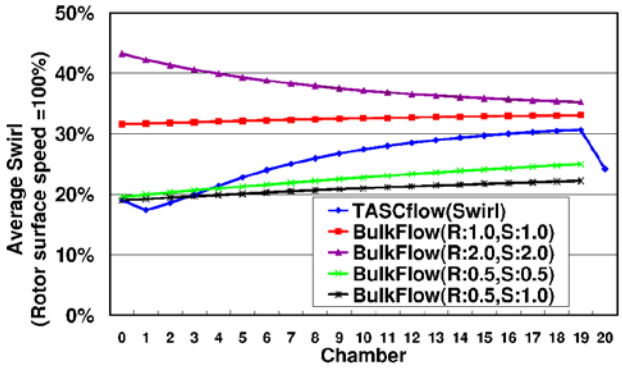

Fig 3 Average swirl for 20 tooth turbine seal [16]

On the whole the results of TASCflow and the bulk flow program do not agree very well for the turbine seal. It may be because the reverse flow in the upstream section is not considered in the bulk flow analysis. The larger swirl would

Copyright © 2016 by ASME

produce a larger tangential force in general so the bulk-flow is more pessimistic in simple terms. The swirl difference was due to a reverse flow in the leak path causing a different boundary condition and in effect the disk wall friction was reduced, producing a smaller tangential swirl. This fact will be discussed in the upcoming additional studies. The conclusion by Hirano was that DYNLAB results were pessimistic for all the conditions studied for the compressor and turbine seal.

The results for the compressor 5 tooth seal were only for an isolated labyrinth seal. Initial attempts to include the gas leak path geometry were not successful due to lack of convergence with the grids selected for evaluation. The isolated seal results were very instructive and the comparison to the bulk flow analysis indicated that the results were conservative and likely suitable for design analysis of high pressure compressors. The ability to predict the inlet swirl of a seal is however, essential for an accurate prediction of rotor system stability. The bulk flow analysis has an estimation of the swirl increase or decrease, depending on geometry of the leak path, and this was the central issue for comparison by Kirk and Guo [17]. The seal geometry was the same and the leak path geometry can be seen in Fig 4.

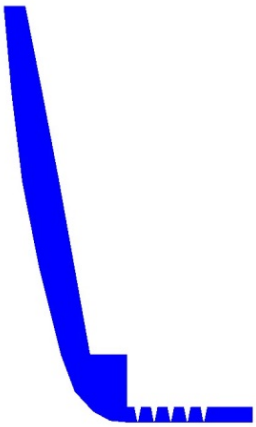

Fig 4 Leak path geometry for the five tooth eye seal [17]

The leak path vector plot and zoom inserts presented in Fig 5 show the predicted complex swirling flows. The chamber flow is similar to the isolated seal results of the previous study [16]. The leak path or channel region shows a division of the leaking flow and the reverse pumping region of the channel. About 60% of the channel has the leaking flow field and the remainder is the reverse pumping flow field. This is contrary to the assumed bulk flow simulation where the disk is assumed to be the surface resisting the leakage flow. This result makes it very clear that the disk friction is not what is resisting the inward flow field, rather a liquid interface. This concept has resulted in a different approach to analysis of the inlet swirl. It is clear that the leak path has less swirl velocity than predicted by a simple inlet bulk-flow. If a reduced leak path width is used with a reduced turbulence friction factor for the disk, then it may be possible to predict the more correct swirling flow.

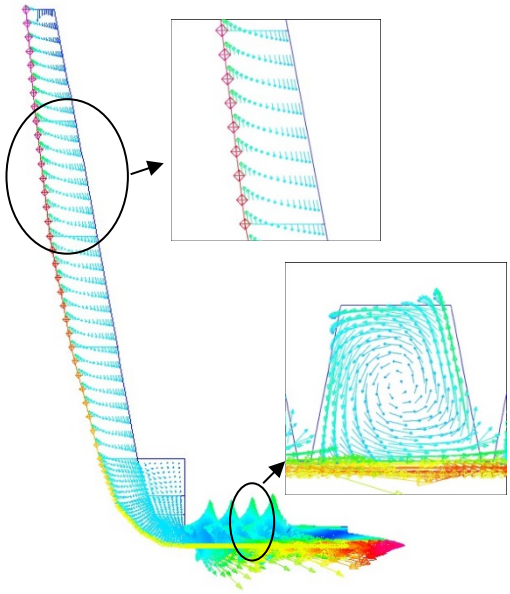

Fig 5 Vector plot for five tooth compressor eye seal [17]

Figure 6 shows that modified disk turbulence factors can reduce the swirl in the labyrinth chambers. The results on this plot have modified rotor surface coefficients as well as different leak path widths. The best result occurs for a 60% leak path width and Yamada rotor coefficients, in the redial chambers, of (nr, mr) equal to (0.085, -0.3) compared to normal values of (0.079. -0.25), while the lowest swirl rates were for the values of (0.120, -0.55). The best solution just below the TASCflow curve is for (0.09, -0.35).

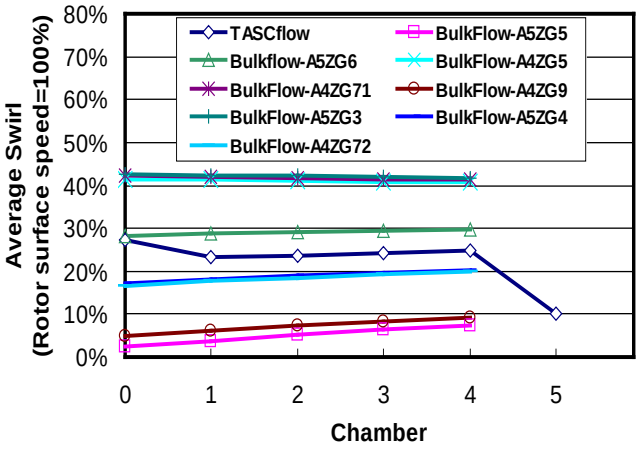

Fig 6 Average swirl in chambers for the five tooth seal [17]

The evaluation of small high speed centrifugal compressor seals is of increasing interest as the application of gas bearing technology to turbocharger type designs are being evaluated for new applications. The same bulk flow analysis can be used for these seals but the concern was for the accuracy of the leakage flows and the swirl predictions. A typical design for a high

Copyright © 2016 by ASME

speed seal is shown in Fig 7. The tooth was a v-notch construction, different from the normal speed standard seal design. This seal was evaluated by TASCflow for the seal alone condition and also for the seal with the inlet leak path or channel. The results were compared to the bulk flow analysis for similar geometry conditions. The dimensions and conditions are provided in Table A-2 in the Appendix. The leakage prediction from TASCflow and comparison to the bulk flow analysis were very similar and the comparison shows much closer agreement for this high speed seal design, with a max of 0.8% difference for the bulk-flow leakage results, compared to 15 % difference for the normal speed compressor seal leakage.

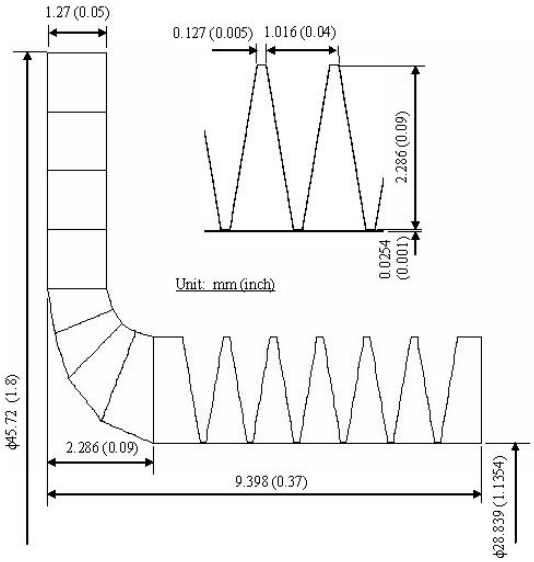

Fig 7 Dimensions of high speed seal and leak path [17]

The prediction of the pressure drop in the seal at the selected design point is presented in Fig 8. The leakage results with and without the leak path channel, are essentially the same and the comparison to the bulk flow analysis is very good. The average swirl in the chambers for the TASCflow results are given in Fig 9. The channel produces a higher swirl in the entry to the seal as would be expected, but the swirls are essentially the same in the seal chambers. The comparison of the bulk flow results are shown in Figs 10 and 11 for the case without and with the channel respectively. It can be seen from these results that it is possible to match very close the swirling flow average tangential velocity by adjusting the disk and rotor friction effects, with the Yamada coefficients of (0.12, -0.55) giving the best result in Fig 11.

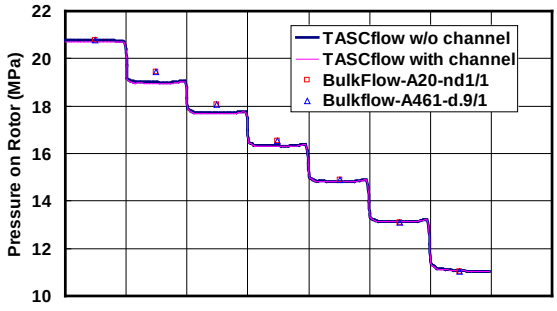

Fig 8 Pressure distribution in axial direction for high speed seal [17]

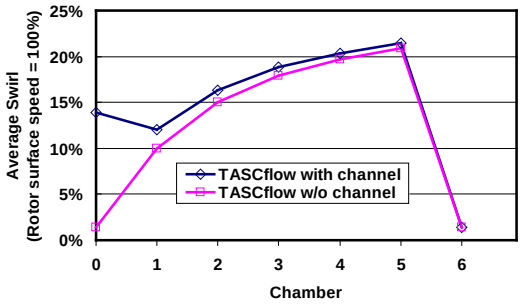

Fig 9 Comparison of average swirl for high speed seal [17]

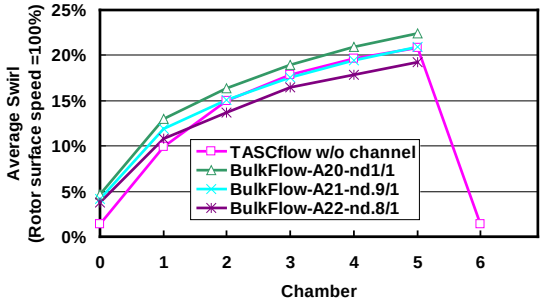

Fig 10 Average swirl high speed seal (without channel) [17]

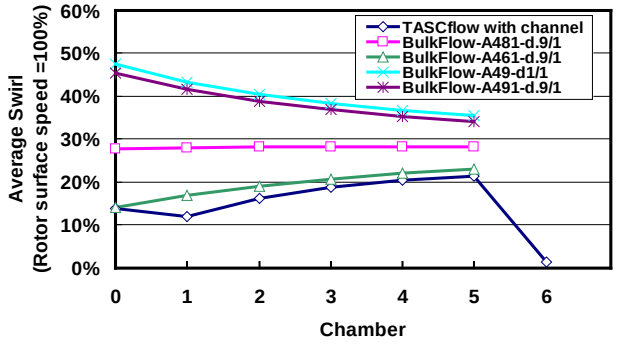

Fig 11 Average swirl high speed seal (with channel) [17]

The vector plot presentation of Fig 12 shows more clearly the inflow and outflow velocity vectors and the chamber

Copyright © 2016 by ASME

swirling and near stagnant flow in the upper portion of the v-notch teeth. The comparison of the bulk flow analysis results for the reduced friction effect and the full disk effect for a tip swirl of 0.6 showed a 23% reduction in the aero excitation due to the reduced disk friction effect and hence less swirl at the seal. For the normal speed study, a 14% reduction in effective aero excitation was achieved as a result of using a reduced friction effect as discussed earlier.

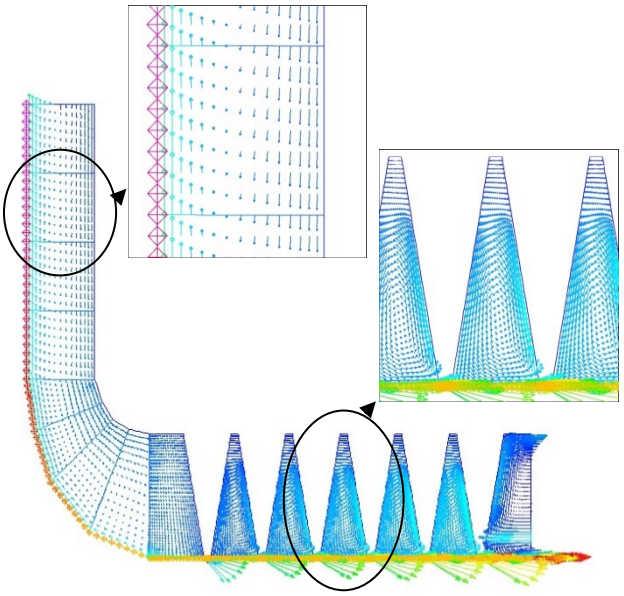

Fig 12 Vector plot for high speed channel and seal [17]

The largest surprise concerning leak path geometry was discovered by the results of the research reported in Kirk and Guo [18]. This paper discusses the influence of leak path friction and geometry on the inlet swirl to the labyrinth seal. A normal speed centrifugal compressor eye seal with various entry channel configurations was considered. Conditions of converging, uniform, and diverging inlets were considered in addition to other variations of friction and entry path design. It was discovered that the average swirl developed as larger for the converging case, and smaller for the diverging case at the very beginning from the impeller tip, which coincide with the initial expectation. However, this relationship flipped at about 30% of the entry channel path and the diverging channel actually displayed the larger average swirl pattern and the converging channel case became smaller. This is opposite to the tentative thought that the converging channel would force more fluid to join the tangential velocity component due to the gradually narrowed path. To explain this phenomenon, the tangential velocity plots and velocity vector profiles were examined (see Fig. 13). From the enlarged subplots of velocity vector of the partial entry channel it was found that the reverse pumping flow decreases when the entry channel changes from the converging, to uniform, and then, to diverging profile.

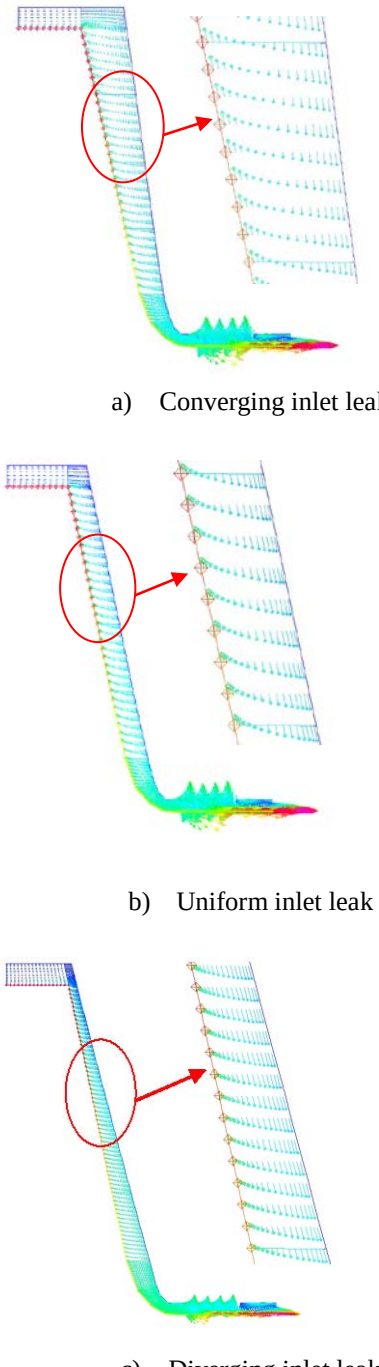

a) Converging inlet leak path

b) Uniform inlet leak path

c) Diverging inlet leak path

Fig 13 Velocity vector plots (converging, uniform and diverging channels for a compressor seal. [18]

This discovery lead to the plan to model all entries by a nearly uniform path with the width in the range of 50% - 80% of the actual inlet width, and to apply a local disk friction to account for the reverse leakage flow in the inlet.

The result in Fig 14 has the bulk flow result shown by the dashed lines and the added F on the label of the case where

Copyright © 2016 by ASME

the disk friction is reduced to account for reverse leakage flow. C is for converging, U is for uniform, and D is for diverging and the 2 is for a double clearance of the usual design condition. The results of bulk-flow compared to CFD are given in Fig 15 for the condition of normal clearance. These results indicate a swirl rate higher in the actual seal. Many other results can be found in Kirk and Guo [18].

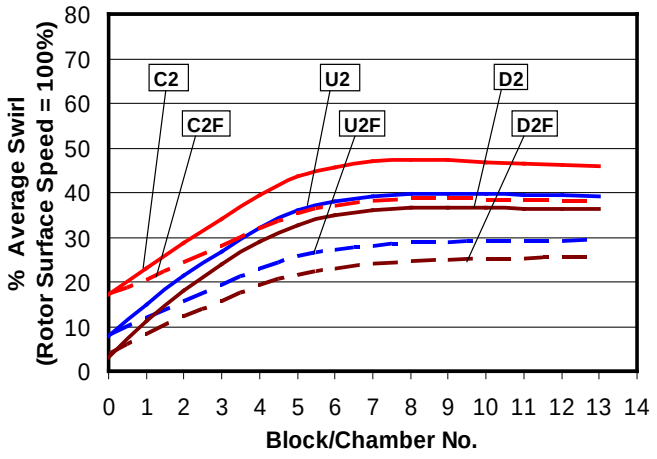

Fig 14 Bulf-flow results of swirl rates along the entire path from tip of impeller. The chamber 9 is just prior to the first tooth of the actual seal. [18]

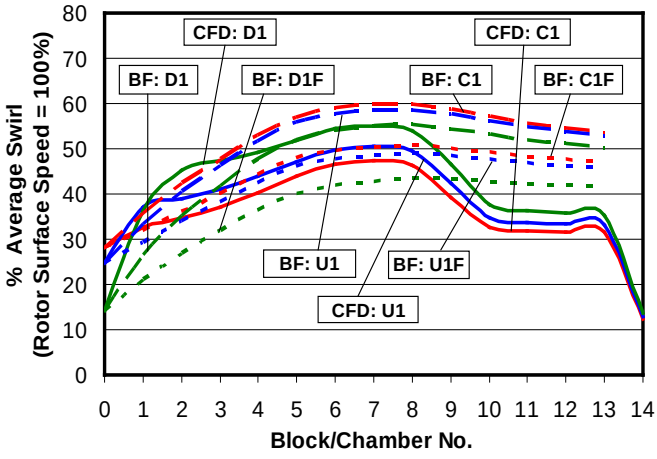

Fig 15 Bulf-flow dashed and CFD solid lines results of swirl rates along the entire path from tip of impeller. The chamber 9 is just prior to the first tooth of the actual seal. [18]

Additional studies of higher, more realistic CFD inlet swirl conditions including balance drum and stepped seals can be found in Kirk and Gao[19] and Gao and Kirk [20]. The comparison of CFX analysis to the bulk-flow analysis for the compressor seal is given in Fig 16a and the comparison of force in radial and tangential direction for Tascflow and CFX is shown in Figs 16- b and 16-c.

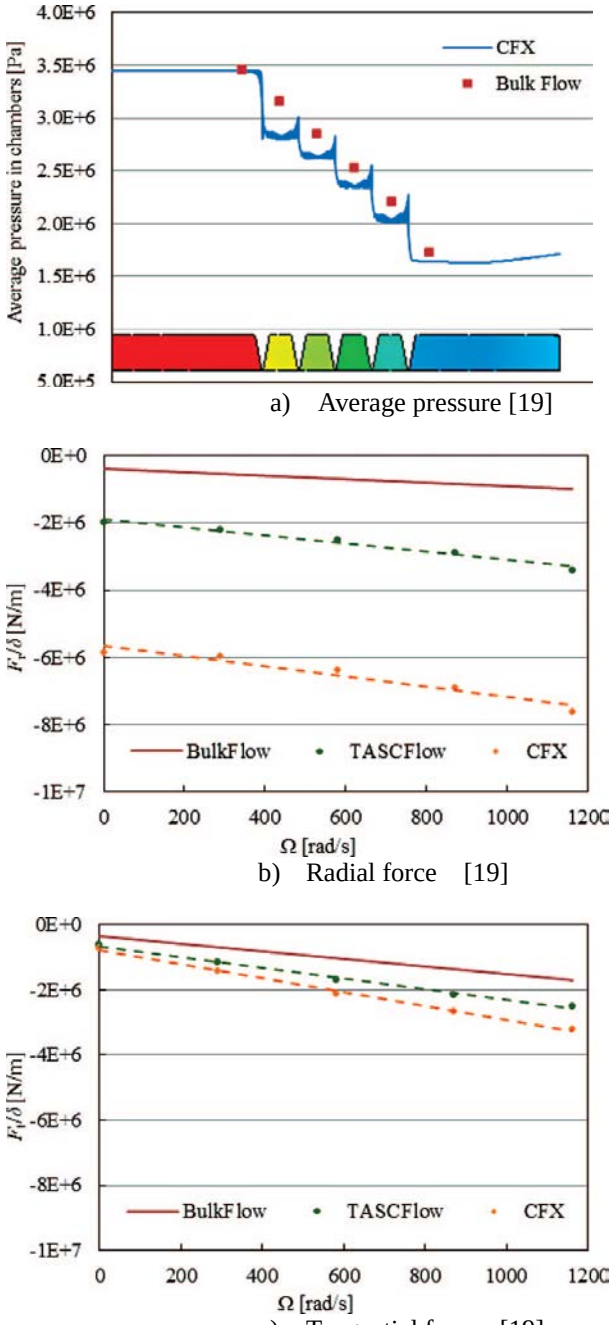

a) Average pressure [19]

b) Radial force [19]

c) Tangential force [19]

Fig16 Comparison of bulk-flow predicted pressure distribution and force levels to TASCflow and CFX.

The comparison of bulk-flow to CFX for pressure distribution of the stepped seal and a balance piston seal is given in Figs 17-a and 17-b. These results show excellent agreement with between CFX and the bulk-flow results.

Copyright © 2016 by ASME

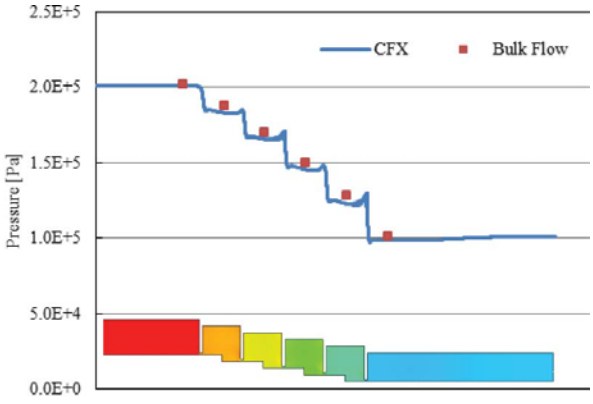

(a) The stepped eye seal

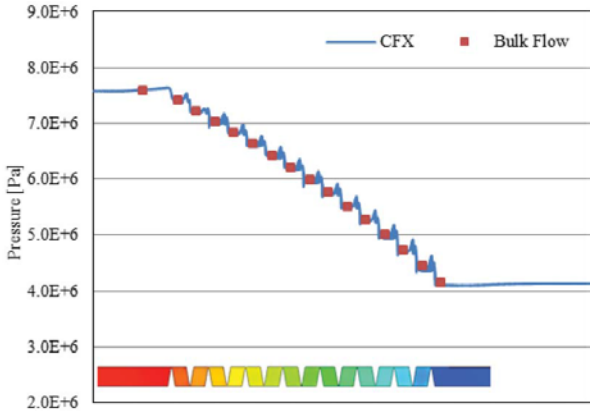

(b) The tooth-interlocking balance drum seal

Fig 17 Comparison of pressure distribution: (a) stepped eye seal and (b) tooth-interlocking balance drum seal. [20]

DISCUSSION OF A NEW DESIGN TOOL

A new user-friendly pre-processor has been developed for the labyrinth seal bulk-flow analysis that makes the data entry much easier for the user. All the features of the original source code are retained in regards to allowing control of the geometry and turbulence parameters to vary tooth to tooth. A one-page entry for the global parameters and links to tables for the tooth geometry variables and turbulence parameters are available on the lower part of this main page. A link to windows for selection of other convergence control variables, multiple speed case option, and a plot of the seal being studied is also available. The bottom of the page is for the output parameters of most interest including the seal dynamic characteristics and leakage plus the effective aero excitation result for the seal. Results for all of the speed cases submitted (up to 10 speed cases per run) are available to view by selecting the different speed cases. The user control is greatly enhanced and the Seal Image option to see the leak path for the given input will allow users to easily assure the seal is correctly entered. This was a major issue in the past.

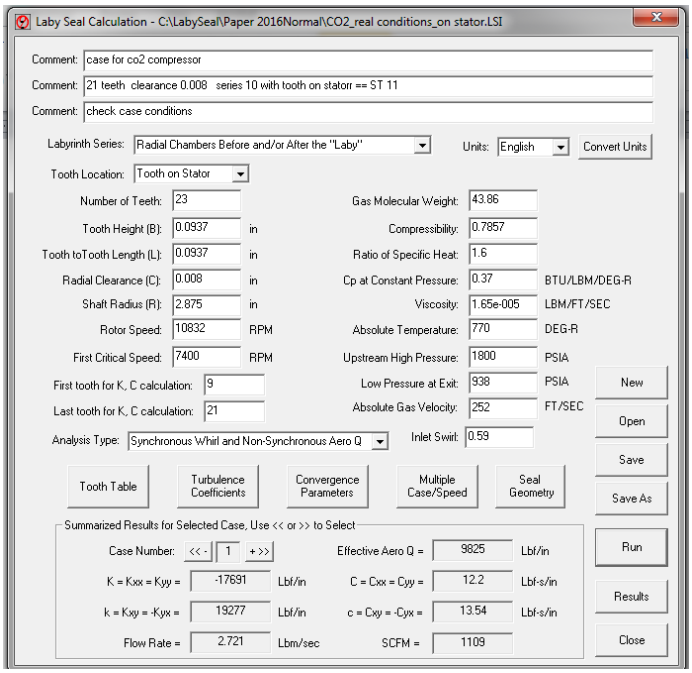

a) Main page of pre-processor

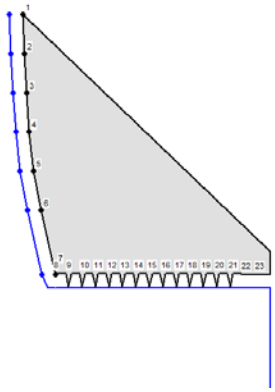

d) Seal Image

b) user control options

c) Options for other inputs or for seal image as in d)

Fig 18 Main page and selected blowups of options

EXAMPLE 1 CASE STUDY

The seal for evaluation is shown in Fig 19 where the leak path is radial from tooth 1 - 6 and axial from 7 – 12. The seal is similar to the normal speed compressor seal with the same conditions and teeth, but the leak path is different. A study was made to examine the influence of the radial disk friction for the reduced friction condition for a 60% width versus the full friction and full width condition. The best case match friction

Copyright © 2016 by ASME

parameters from the Fig 6 results were used for this study and the results are summarized in Table 1.

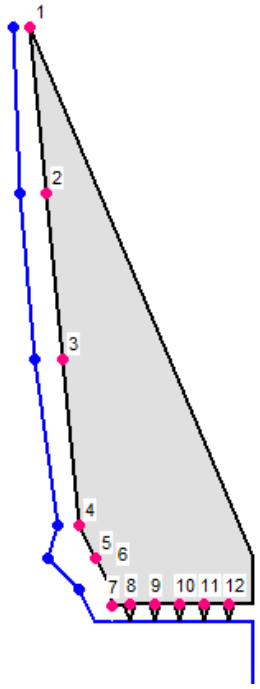

Fig 19 Seal for example case 1 study

Table 1 Selected results from Example Case 1 Study

case	Tip swirl + Flow Corr.	Swirl Prior to tooth 8	Q eff ratio	Flow ratio
1	0 + FC 1	0.34	- 0.37	1.12
2	0.6+ FC 1	0.65	0.797	1.01
3	0 + FC 1.05	0.33	- 0.40	1.17
4	0.6+ FC 1.05	0.66	0.78	1.06
5	0 + FC 1	0.47	0.12	1.1
6	0.6 + FC 1	0.7	1	1
7	0 + FC 1.06	0.46	.06	1.17
8	0.6+ FC 1.06	0.71	0.92	1.06
9	0.6+ FC 0.5	.61	1.6	0.508

Case 1–4 = narrow leak path and reduced disk friction
Case 5–9 = full width leak path, full turbulence
Qeff reference 2079 lb/in ; Flow reference = 1562 SCFM

For the results reported in Table 1 the case 6 condition is used as the reference value for Qeff and flow to allow easier comparison of the influence of the different conditions. It is clear the exit flow is influenced by the inlet swirling flow and the effective aerodynamic instability mechanism changes from negative for narrow inlet and zero swirl at the tip of the impeller to large numbers when the tip fluid swirl is increased to 60% of the surface speed. This value of tip swirl is typical for almost all centrifugal compressor stages with backward leaning vanes. A 20 % reduction in aero excitation is noted for the use of reduced friction on the radial disk portion of the leak path. This is great for matching CFD results but a designer would likely prefer to take the worst case condition and use that to design the compressor.

EXAMPLE 2

For a second example a balance drum seal using CO_2 was evaluated for different teeth placement: on stator, on rotor, and interlocking. The seal geometry is given in Appendix A, and the properties are given in Fig 18-a.

Table 2 Selected results for the CO_2 gas seal of example 2

Teeth location	Qeff lb/in	N /mm	SCFM	kg/s
On stator	9825	1720	1109	1.23
On rotor	5193	909	1146	1.27
Interlocking	5881	1030	579	0.64

The take away here is that the interlocking design gives the lowest leakage flow and lower effective aerodynamic excitation than the tooth on stator design. See Table A-3 for lower disk friction results to compare to Table 2.

CONCLUSIONS

This paper gives a summary of the work on CFD analysis of compressor labyrinth seals conducted from 2003 – 2013 at the Virginia Tech Rotor Dynamics Lab. In most cases, the results were compared to the bulk-flow analysis for leakage and aero excitation or Q effective as defined by Eq (2). The results show that for normal speed machines and high speed machines, the bulk-flow analysis prediction of destabilizing forces are in most all cases higher than the effects predicted by CFD analysis. The most important points of the results are summarized as follows:

1. The bulk-flow analysis produces results that are conservative for evaluation of labyrinth seals for rotating machinery.
2. The shape of the leak path prior to the seal can greatly influence the results for both leakage and Q effective.
3. The bulk-flow prediction for a converging leak path will over-estimate the seal inlet swirl compared to CFD analysis results.
4. The bulk-flow prediction for a diverging leak path will under-estimate the seal inlet swirl compared to CFD analysis results.
5. CFD results show that reverse flow created by the rotating disk portion of the inlet will make both the converging and diverging inlets behave as a more uniform path with a reduced effective width.

Copyright © 2016 by ASME

6. A suggested design approach is to use the minimum width of the inlet leak path as the effective width of the radial portion of the leak path.
7. To be conservative use the standard turbulence factors for both the rotor and stator (0.079, -0.25).
8. A lower limit estimation of the Q effective for the seal can be made by using modified turbulence coefficients for the radial portions of the leak path.
9. This research suggests that modified Yamada coefficients of (0.085, -0.30) – (0.09, -0.35) be used in place of the standard values (0.079, -0.25) for the radial disk portion of the leak path for a better match to CFD.
10. The seal chambers should be modelled to give the approximate flow area of the chambers. It is suggested to use the actual tip to tip spacing with an effective tooth height to approximate the area of the chamber cross-section.

ACKNOWLEDGMENTS

The CFD results presented in this paper were produced by Toshoi Hirano, Dr. Zenglin Guo, and Dr. Rui Gao while working as research assistants at the Virginia Tech Rotor Dynamics Lab.

REFERENCES

[1] Iwatsubo, T., 1980, "Evaluation of Instability Forces of Labyrinth Seals in Turbines or Compressors," Proc. Rotordynamic Instability Problems in High Performance Turbomachinery, NASA CP-2133, Texas A&M University, pp139-167.

[2] Childs, D. W. and Scharrer, J. K., 1986, "An Iwatsubo-Based Solution for Labyrinth Seals: Comparison to Experimental Results," *Journal of Engineering for Gas Turbines and Power*, **108**(2), pp 325–331.

[3] Childs, D.W. and Scharrer, J. K, 1986, "Experimental Rotordynamic Coefficient Results for Teeth-on-Rotor and Teeth-on-Stator Labyrinth Gas Seals," *Journal of Engineering for Gas Turbines and Power*, **108**(4), pp 599–604.

[4] Scharrer, J. K., 1987, "Theory versus Experiment for the Rotordynamic Coefficients of Labyrinth Gas Seals: Part I – A Two control Volume Model," Proc. ASME 11th Biennial Conference on Mechanical Vibration and Noise, Rotating Machinery Dynamics Volume Two, pp411-426

[5] Childs, D.W., Scharrer, J. K., 1987, "Theory versus Experiment for the Rotordynamic Coefficients of Labyrinth Gas Seals: Part II – A Comparison to Experiment," Proc. ASME 11th Biennial Conference on Mechanical Vibration and Noise, Rotating Machinery Dynamics Volume Two, pp427-434.

[6] Kirk, R. G., 1988, "Evaluation of Aerodynamic Instability Mechanisms for Centrifugal Compressors Part I:Current Theory," *ASME Journal of Vibration, Acoustics, Stress, and Reliability in Design*, Vol. 110, No. 2, April, pp. 201-206.

[7] Kirk, R. G., 1988, "Evaluation of Aerodynamic Instability Mechanisms for Centrifugal Compressors – Part II: Advanced Analysis," Journal of Vibration, Acoustics, Stress and Reliability in Design, **110**(2), pp. 207-212.

[8] Kirk, R. G., 1990, "A Method for Calculating Labyrinth Seal Inlet Swirl Velocity," ASME J. Vibration and Acoustics, **112**(3), pp. 380-383.

[9] Kirk, R. G., K.V.S. Raju, and K. Ramesh, 1999, "PC-Based Analysis of Turbomachinery Vibration," The Shock and Vibration Digest, **31**(6), pp 449-454.

[10] Rhode, D. L., Hensel, S. J., Guidry, M. J., 1992,"Labyrinth Seal Rotordynamic Forces Using a Three-Dimensional Navier-Stokes Code," ASME J. of Tribology, **114**, pp.683-689

[11] Rhode, D. L., Hensel, S. J., Guidry, M. J., 1993, "Three-Dimensional Computations of Rotordynamic Force Distribution In a Labyrinth Seal," STLE Tribology Transaction, **36**(3), pp461-469

[12] Ishii, E., Kato, C., Kikuchi, K., and Ueyama, Y., 1997, "Prediction of Rotordynamic Forces in a Labyrinth Seal Based on Three-Dimensional Turbulent Flow Computation," JSME International Journal, Series C, **40**(4**)** pp. 743-748.

[13] Kwanka, K., Sobotzik, J. and Nordman, R., 2000, "Dynamic Coefficients of Labyrinth Gas Seals A Comparison of Experimental Results and Numerical Calculations," ASME International Gas Turbine and Aeroengine C ,ngress & Exhibition, 2000-GT-403.

[14] Moore, J. J., 2003, Three-dimensional CFD Rotor-dynamic Analysis of Gas Labyrinth Seals, *Journal of Vibration and Acoustics, Trans. ASME,* 125(3), 427-433.

[15] Guo Z, Hirano T and Kirk R. G., 2005,"Application of CFD Analysis for Rotating Machinery, Part 1: Hydrodynamic, Hydrostatic Bearings and Squeeze Film Damper," *Journal of Engineering for Gas Turbines and Power, Trans. ASME*, 127, 445-451.

[16] Hirano T., Guo, Z. & Kirk R.G., 2005, "Application of CFD Analysis for Rotating Machinery, Part 2: Labyrinth Seal Analysis," *Journal of Engineering for Gas Turbines and Power, Trans. ASME*, 127, 820-826.

[17] Kirk R.G. and Guo, Z., 2004,"Calibration of Labyrinth Seal Bulk Flow Design Analysis Prediction to CFD Simulation Results," In *Proc. IMechE Eighth International Conference on Vibrations in Rotating Machinery*, Swansea, UK.

[18] Kirk, R. G. and Guo, Z., 2009, "Influence of Leak Path Friction on Labyrinth Seal Inlet Swirl," *Tribology Transactions*, **52**(2), pp 139–145.

[19] Kirk, G. and Gao, R., 2012, "Influence of Pre-swirl on Rotordynamic Characteristics of Labyrinth Seals," STLE Tribology Transactions, 55(3), pp 357-364.

[20] Gao, R. and Kirk, G., 2013 ,"CFD Study on Stepped and Drum Balance Labyrinth Seal," Tribology Transactions, 56:4, 663-671.

 Copyright © 2016 by ASME

APPENDIX A

PARAMETERS FOR SEALS

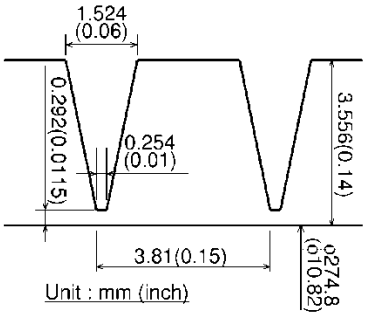

Tooth profile for normal speed compressor seal

Tooth	R	B	C	L
1	4.78120	0.00010	0.09370	0.01000
2	4.50890	0.00010	0.09370	0.01500
3	4.23660	0.00010	0.09370	0.02000
4	3.96430	0.00010	0.09370	0.03000
5	3.69200	0.00010	0.09370	0.05000
6	3.41970	0.00010	0.09370	0.10000
7	2.97000	0.00010	0.09370	0.04500
8	2.87500	0.00010	0.10000	0.09370
9	2.87500	0.09370	0.00800	0.09370
10	2.87500	0.09370	0.00800	0.09370
11	2.87500	0.09370	0.00800	0.09370
12	2.87500	0.09370	0.00800	0.09370
13	2.87500	0.09370	0.00800	0.09370
14	2.87500	0.09370	0.00800	0.09370
15	2.87500	0.09370	0.00800	0.09370
16	2.87500	0.09370	0.00800	0.09370
17	2.87500	0.09370	0.00800	0.09370
18	2.87500	0.09370	0.00800	0.09370
19	2.87500	0.09370	0.00800	0.09370
20	2.87500	0.09370	0.00800	0.09370
21	2.87500	0.09370	0.00800	0.09370

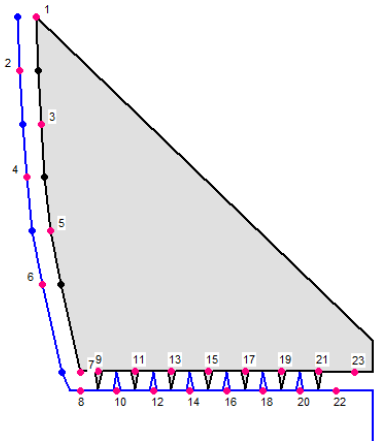

Example 2 properties

Table A-1 Normal speed compressor eye seal

Rotor Diameter	274.8 mm (10.82 ”)
Clearance at Teeth	0.292 mm (0.0115 ”)
Number of teeth	5
Rotation Speed	1162 rad/s (11,097 rpm)
Inlet Pressure	3.447 MPa (500 psi)
Outlet Pressure	1.724 MPa (250 psi)
Inlet Temperature	366.7 K (660 R)
Inlet Swirl	0
Flow	Compressible, Turbulent k-ε Scalable Log Law wall function
Fluid	Air (Ideal gas)

Table A-3 results for the CO2 gas seal of example 2, with disk friction reduced as suggested in conclusions (0.085, -0.3)

Teeth location	Qeff lb/in	N /mm	SCFM	kg/s
On stator	8999	1576	1113	1.24
On rotor	4554	798	1149	1.28
Interlocking	4643	813	584	0.65

Table A-2 High speed compressor eye seal

Rotor Diameter	28.839 mm (1.1354 in.)
Clearance at Teeth	0.0254 mm (0.001 in.)
Number of Teeth	6
Eccentricity ratio	10% of Tip Clearance
Rotation Speed	100,000 RPM (10,466.7 rad/s)
Inlet Pressure	20.765 MPa (3011.7 psi)
Outlet Pressure	11.030 MPa (1599.8 psi)
Inlet Temperature	366.7 K (660 R)
Inlet Swirl	0

Copyright © 2016 by ASME